ELSEVIER

Thin Solid Films 279 (1996) 145–154

thin solid films

Characteristics of the thermal oxidation of heavily boron-doped polycrystalline silicon thin films

M. Boukezzata [a], D. Bielle-Daspet [b], G. Sarrabayrouse [b], F. Mansour [a]

[a] *Institut d'Electronique, Université de Constantine, Route de Ain El-Bey, 25 000 Constantine, Algérie*

[b] *LAAS du CNRS, 7, Avenue du Colonel Roche, 31077 Toulouse Cédex, France*

Received 23 March 1995; accepted 6 October 1995

Abstract

Dry oxidation kinetics were compared for 2×10^{20} cm^{-3} boron-implanted and in-situ doped films deposited at temperatures ranging between 520 and 620 °C. The characteristics of the thermal oxidation of these films have been studied over the oxidation temperature range of 750 to 1 050 °C and for durations of 10 min to 26 h. High values of both the surface oxidation rate k_s and the oxide diffusion coefficient D are evidenced as typical of the in-situ doped films.

In addition to the well-known effect that heavy doping increases the rate of oxidation similar to what is observed in single-crystal silicon, it is also shown specially, for the in-situ boron-doped films compared with 2×10^{20} cm^{-3} in-situ phosphorus-doped ones, that the greatest oxidation rate is observed at high oxidation temperatures ($T_{ox} > 1\,000$ °C). This enhancement is related to some specific factors of these materials, such as grain boundary structures, defects, texture and electrical properties related to the segregation and supersaturation phenomenon which occur at these levels of doping.

Keywords: Oxidation; Chemical vapour deposition; Boron; Silicon; Ion implantation

1. Introduction

More accurate and careful understanding of the behaviour of heavily boron-doped polycrystalline silicon thin films (p-type low-pressure chemical vapour deposition (LPCVD)-Si) during deposition and post-deposition process steps has been the subject of several studies during the last years. An extensive investigation is necessary for processing of power devices and integrated circuits. Particularly, these films are widely used as interconnections, resistors which are independent of operating voltage, floating gates in EPROM and EEPROM memories or a diffusion source to form junctions in metal-oxide semiconductor integrated circuits and CCDs [1,2]. In many of these applications, polysilicon films are subjected to thermal-oxidation treatment under an oxygen ambient. As a result, many devices and integrated circuit properties could be influenced by this process cycle. Several authors have studied the thermal oxidation kinetics of n-type polysilicon films under wet, steam or dry oxygen [2,3]. While, however, the major problems of the oxidation behaviour of single-crystal silicon were resolved and several models are described and reported in the literature [4–9], on the contrary, only few attempts were devoted to understanding the kinetics of the process in polysilicon thin films and the influence of material structure and electronic properties on the oxidation behaviour. Within this scope, the aim of this work is to give a precise knowledge of the oxidation kinetics of specially heavily boron-doped layers (p-type) and of the influence of the doping mode (in-situ doping method or implantation).

2. Experimental procedure

This study deals with ≈200 nm thick films, isothermally deposited in industrial reactors of many important manufacturers, at temperatures T_d ranging between 520 and 620 °C, on bare or oxidized (200 nm thermal oxide) silicon wafers. These substrates are used with 100 or 125 mm diameter and resistivity ρ varied from 10 to 22 Ω cm. The oxidation in dry oxygen for temperatures T_{ox} from 750 to 1050 °C and durations t_{ox} of 10 min to 20 h (50 °C min^{-1} up and down ramping under dry oxygen) is investigated for the following four deposited series.

SSDI 0040-6090(95)08172-0

1. 2×10^{20} cm^{-3} in-situ doped films (B-LPCVD series) were deposited in the industrial furnaces of Motorola (Toulouse, France), from the gaseous mixture 3% SiH_4–BCl_3–N_2. The pressure was set at 400 mTorr and the temperature T_d ranged from 520 to 605 °C.
2. Undoped films (U-LPCVD series), manufactured by Semy Engineering (Montpellier, France) were deposited at T_d=520–620 °C, from a mixture gas of SiH_4–N_2/H_2 under a pressure of 200 mTorr.
3. Films of the above U-LPCVD series were implanted with 10^{16} cm^{-2} boron atoms at 40 KeV using the ion-implantation equipment belonging to the Automatic and Architectural Systems Laboratory (LAAS of CNRS, France). These films will be labelled as the B_i-LPCVD series, which correspond to boron contents of $\approx2\times10^{20}$ cm^{-3} within the film.
4. A 5×10^{20} cm^{-3} in-situ phosphorus-doped film (P-LPCVD series) was also deposited in the industrial reactors of Semy Engineering (Montpellier, France) at temperature ranging from 520 to 620 °C from a gas mixture of SiH_4–PH_3 diluted in H_2 under a pressure of 700 mTorr. This last series was realized with an opposite nature of dopant (n-type) and will be compared with the boron-doped (p-type) and the undoped oxidation properties films.

Lightly doped monocrystalline silicon labelled as T⟨100⟩, T⟨111⟩ (ρ= 14–22 Ω cm which corresponds to a level doping from 6×10^{14} to 1.5×10^{15} cm^{-3}) and heavily implanted $T\langle100\rangle_i$, $T\langle111\rangle_i$ (10^{16} cm^{-2} boron dose at 40 KeV which gives a resistivity ρ=0.01 Ω cm and, therefore, a doping level around 5×10^{19} to 1×10^{20} cm^{-3}) are systematically used in the experiments as control samples.

Oxide thicknesses W_{ox} were obtained from mechanical-step measurements using a talystep profilometer (Taylor–Hobson 1661) with ±5 nm accuracy. The variations of W_{ox} with t_{ox} and T_{ox} were analysed by comparing the experimental results with those reported in Ref. [10] from Deal and Grove [6], Naïto et al. [7] and Han and Helms [8] models. The initial oxide thicknesses W_i were estimated from measurements after an up and down thermal ramping.

Also, surface roughness using Raman scattering spectroscopy at 480 nm, four-point probe resistivity measurements and transmission electron microscopy (TEM) observations (200 KeV Temscan microscope) of the polysilicon remaining layer after stripping off the grown oxide SiO_2 were performed. The details of these experimental techniques are described in the literature [11,12,14].

3. Results

3.1. General features of the film oxidation

The obtained results of kinetics oxidation are illustrated in the figures given below. We can see the following.

1. For the in-situ boron-doped layers and for the same oxidation temperature T_{ox}, the thicker oxides are grown at the lower T_d (see Fig. 1). First, we note that the oxide thickness varies inversely proportional to the variation of the deposition temperature T_d and that the oxidation rates of these layers are always higher than the control sample ones. Second, when T_{ox} changes (see Fig. 2) these observations remain the same. The only difference (see Fig. 3) is the discrepancy of the oxidation rate between the lowest and the highest T_d. This behaviour will be discussed in the following sections. Moreover, these films clearly have higher oxidation rates than the boron-implanted or undoped films as shown in Fig. 4, as opposed to the boron-implanted case.

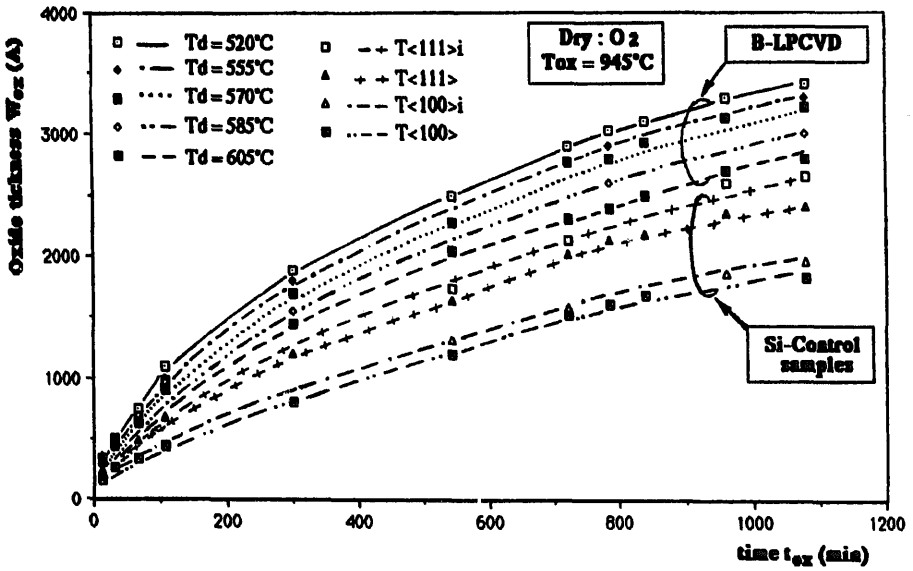

Fig. 1. Evolution of the average oxide thickness W_{ox} as a function of oxidation time t_{ox} for the 200 nm B-LPCVD layers for the oxidation temperatures T_{ox} = 945 °C for the all deposition temperatures T_d = 520, 555, 570, 585 and 605 °C and for control samples T⟨100⟩, T⟨111⟩, $T\langle100\rangle_i$, and $T\langle111\rangle_i$.

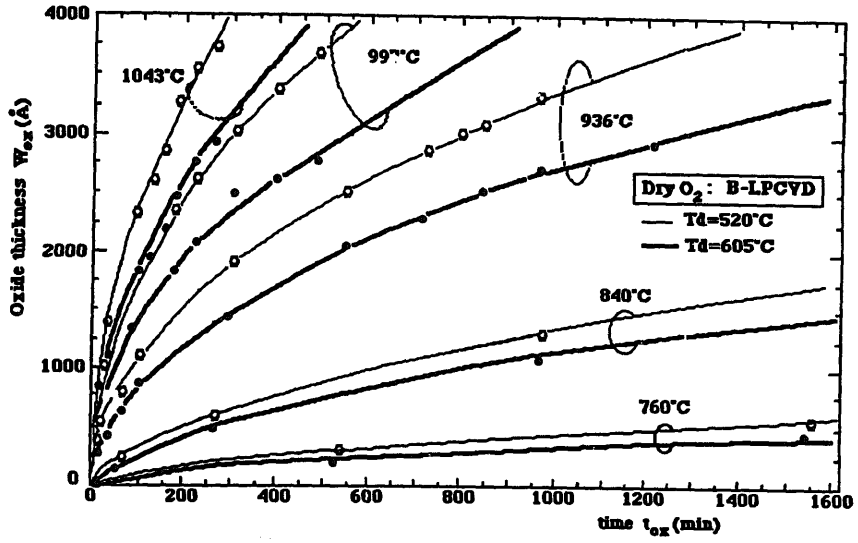

Fig. 2. Evolution of the average oxide thickness W_{ox} as a function of oxidation time t_{ox} for the 200 nm B-LPCVD layers for the five oxidation temperatures T_{ox} = 760, 840, 936, 997 and 1 043 °C for the extremal deposited temperatures T_d = 520 °C (———) and T_d = 605 °C (———).

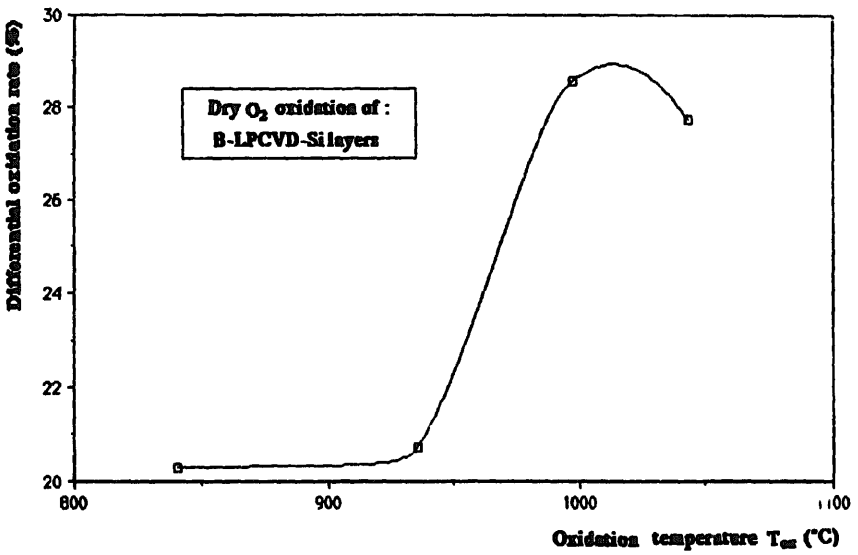

Fig. 3. Variation of the differential of the oxidation rates (DOR) versus T_{ox} for the 200 nm B-LPCVD silicon films.

2. The oxidation rates of the four layers (B-, B_i-, U- and P-LPCVD series) vary with T_d as illustrated in Fig. 5 and Fig. 6. Again, the strongest variations are observed with the B-doped films, and specially the in-situ doped ones.
3. The in-situ boron- and phosphorus-doped layers present only a different behaviour at high oxidation temperature $T_{ox} > 1\,000$ °C, (see Fig. 6(a)); whereas, at low oxidation temperature $T_{ox} < 1\,000$ °C, (Fig. 6(b)) both of the layers give the same results.

If we determine the amount differential of the oxidation rate (DOR) from Fig. 2 for each temperature T_{ox}, we obtain:

$$\mathrm{DOR}(\%) = \frac{R_{520} - R_{605}}{R_m} \times 100 \qquad (1)$$

where R_{520} is the oxidation rate of layers deposited at T_d = 520 °C, R_{605} is the oxidation rate of layers deposited at T_d = 605 °C, and R_m denotes the mean value between the two rates. We can see (Fig. 3) that this phenomenon increases with T_{ox} until T_{ox} reaches a temperature of 1 000 °C, and then, decreases

4. By comparison, the type of the substrate, either bare or oxidized Si wafer, whose influence was specially investigated for the shortest oxidations, has appeared to be of negligible effect. Consequently, the following results concern only deposits on oxidized substrates.

3.1.1. Microstructural analysis

The thermal-oxidation features reported above and particularly those observed on heavily boron-doped LPCVD silicon films appear to correlate with the structural properties of

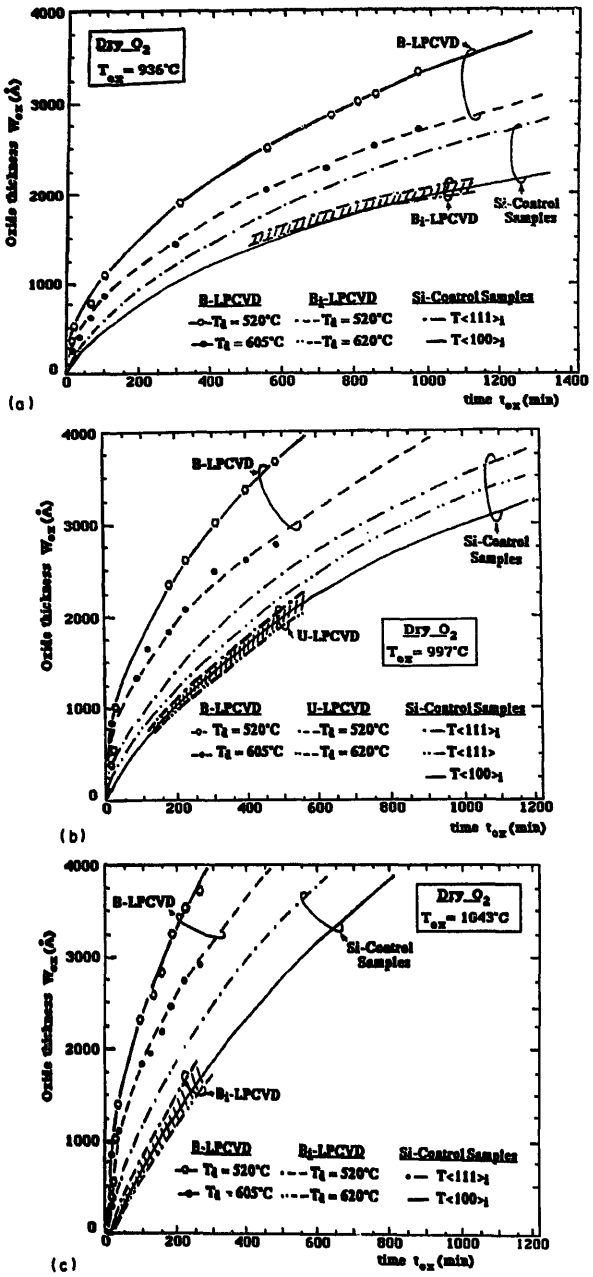

Fig. 4. Variations of the oxide thickness W_{ox} as function of oxidation time t_{ox} for the 200 nm B-LPCVD layers compared with the: B_i-LPCVD associated with a lightly doped and implanted (10^{16} cm^{-2} B, 40 KeV) monocrystalline control samples noted T⟨100⟩, T⟨111⟩, T⟨100⟩$_i$, and T⟨111⟩$_i$ oriented silicon for the extreme deposited temperatures T_d = 520 °C and T_d = 605 °C and for the oxidation temperatures: (a) T_{ox} = 936 °C, (b) T_{ox} = 997 °C, (c) T_{ox} = 1 043 °C.

these layers which were the subject of many studies, most of their results having been published elsewhere [11]. The variations of microstructure with T_d and dopant were characterized by TEM observations, reflection high-energy electron diffraction (RHEED) diffractions, cross-sectional examinations, and optical means [7,8,13,14] on the as-grown, undoped, boron-doped and phosphorus-doped LPCVD silicon films. Most of the results obtained reveal the effect of dopant on the film microstructure and thus, on the crystallization mechanisms. Indeed, it is well-known now that the film microstructures of these layer series and their variations versus T_d are quite different. For the as-grown, undoped films, when T_d increases from 520 to 605–620 °C, the microstructures change from clearly the amorphous state to the poly-

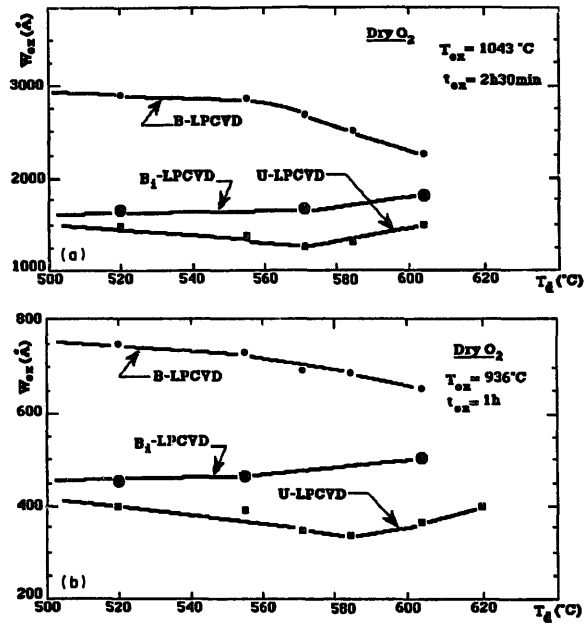

Fig. 5. Oxide thicknesses W_{ox} versus the deposition temperature T_d of the three layers B-, B_i- and U-LPCVD for a dry oxidation at: (a) T_{ox} = 1 043 °C (2 h 30 min), (b) T_{ox} = 936 °C (1 h).

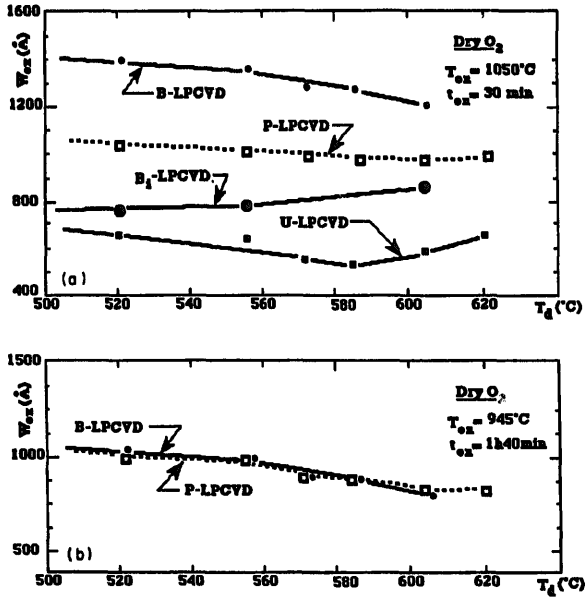

Fig. 6. Oxide thicknesses W_{ox} vs. the deposition temperature T_d of the in-situ boron-doped (B-LPCVD), boron-implanted (B_i-LPCVD) and undoped (U-LPCVD) layers compared with the in-situ phosphorus-doped layers (P-LPCVD) for a dry oxidation at: (a) T_{ox} = 1 050 °C (30 min), (b) T_{ox} = 945 °C (1 h 40 min).

Table 1
Comparison between the mean grain sizes of TEM, Raman measurements and calculated data for the as-grown and B-LPCVD silicon films annealed at T_{ox} = 840, 940 and 1 050 °C for the extreme deposited temperatures T_d = 520 and 605 °C

T_{ox} (°C)	t_{ox}	T_d = 520 °C			T_d = 605 °C		
		$\langle G\rangle_{TEM}$ (nm)	$\sigma_{\alpha Raman}$ (nm)	$\langle G\rangle_{rel.(2)}$ (nm)	$\langle G\rangle_{TEM}$ (nm)	$\sigma_{\alpha Raman}$ (nm)	$\langle G\rangle_{rel.(2)}$ (nm)
840	1 h	80	3	52	40	3	27
840	16 h	85	3	75	60	3	31
940	12 min	90	4	60	70	5	51
940	1 h 46 min	–	4	66	–	5	58
940	13 h	100	4	81	100	5	75
1 050	12 min	100	3	92	80	5	82
1 050	1 h 30 min	140	3	129	200	5	182
1 050	4 h	–	3	–	–	5	–
As grown		80	3	40	40	3	20

crystalline. It is stated that as-grown, U-LPCVD silicon films are amorphous as their average grain size is 20–30 nm. Actually, they are polycrystalline, an amorphous state having a much shorter range of order (only the first neighbours around a silicon atom are at the same distance as in crystalline silicon). On the contrary, all as-grown in-situ boron-doped films are polycrystalline even at the lowest temperature T_d. But their crystalline grain size decreases and falls off from 100 nm at T_d = 520 °C to around 40 nm at T_d = 605 °C, while the crystalline quality of these grains increases. Crystalline quality means that the average grain size tends to becomc small and uniform, while the number of the grains increases tremendously but with a low defect density, whereas the phosphorus-doped LPCVD silicon films exhibit microstructures similar to those of boron-doped films. However, we observe that those grown at T_d = 520 °C are amorphous, they are partially polycrystalline when grown at T_d = {570–585 °C} and then, totally polycrystalline when grown at higher temperature (T_d = {605–620 °C}).

Obviously, these differences appear at the very beginning of the film growth. Thus, it must be noticed that, as for the B-LPCVD films, the nucleation of c-Si grains in P-LPCVD films occurs at the gas–film interface. On the contrary, cross-sectional examinations of U-LPCVD silicon films show an opposite behaviour. The nucleation of crystalline grains occurs at the film–substrate interface; the film microstructure then depends on the relative magnitude of the c-Si growth rate and the film deposition rate [11]. Consequently, we believe that this evolution of microstructure is due to the evolution of the nucleation rate which is, a priori, proportional to boron atom concentration, and to the evolution of the deposition rate. When the product of nucleation rate by deposition rate decreases, the grain size or the defect density decreases, leading to a higher crystalline quality. A correlation was also established between the grain size given by Raman experiments and TEM examinations. In Table 1, the values of the mean grain sizes deduced from the two methods are presented. We can see a large mutual disagreement. This difference can be explained by the fact that the meanings of these grain sizes are also quite different. For the first method, the apparent low Raman grain size corresponds well to the mean size of crystal domains free of defects such as grain boundaries, twins, subgrain boundaries, and dislocation networks. Thus, the increase with T_d in the Raman grain size indicates that the crystal perfection increases as T_d increases, while the TEM grain size values were mainly related to the variations in the nucleation rate but not to the defect density.

3.1.2. Electrical measurements

We cannot fully explain the oxidation behaviour of polysilicon without taking into account the presence of grains and grain boundaries, which can markedly change the electrical properties and therefore can also play a significant role in the oxidation behaviour. These electrical properties have been studied through the film sheet resistivity, which is mainly measured by the Hall effect and the four-point probe measurements.

With the Hall mobility μ_H deduced from the resistivity measurements and using the published values of the mobility in the grain μ_G from Refs. [15,16], μ_G is assumed to be equal to the monocrystalline silicon value (60 $cm^2\ V^{-1}\ s^{-1}$: this value corresponds very well to our experiment conditions). From the relationship given below [1,17]:

$$\langle G\rangle = k\left(\frac{\mu_G - \mu_H}{\mu_G \mu_H}\right)^{\alpha} = k(\mu_{GB})^{\alpha} \qquad (2)$$

where, $k = 1.22 \times 10^{-8}$ and $\alpha = -1.7$, we can quantitatively evaluate the mean grain size $\langle G\rangle$. We report again in Table 1 the values obtained together with those deduced from TEM and Raman scattering measurements. On the whole, we can note a good qualitative agreement between the results measured by TEM and those calculated with Eq. (2), but not with Raman measurements. This disagreement, however, is only apparent, and can be explained taking into account the differences between the two methods, such as we have previously mentioned and attempted to clarify just above.

As a consequence of oxidation, the surface roughness of these 200 nm thick deposits clearly increases above its common as-grown value of $(\sigma_\alpha) < 5$ nm up to the maximum value $(\sigma_\alpha)_{max} = 10$ nm in the case of the undoped films

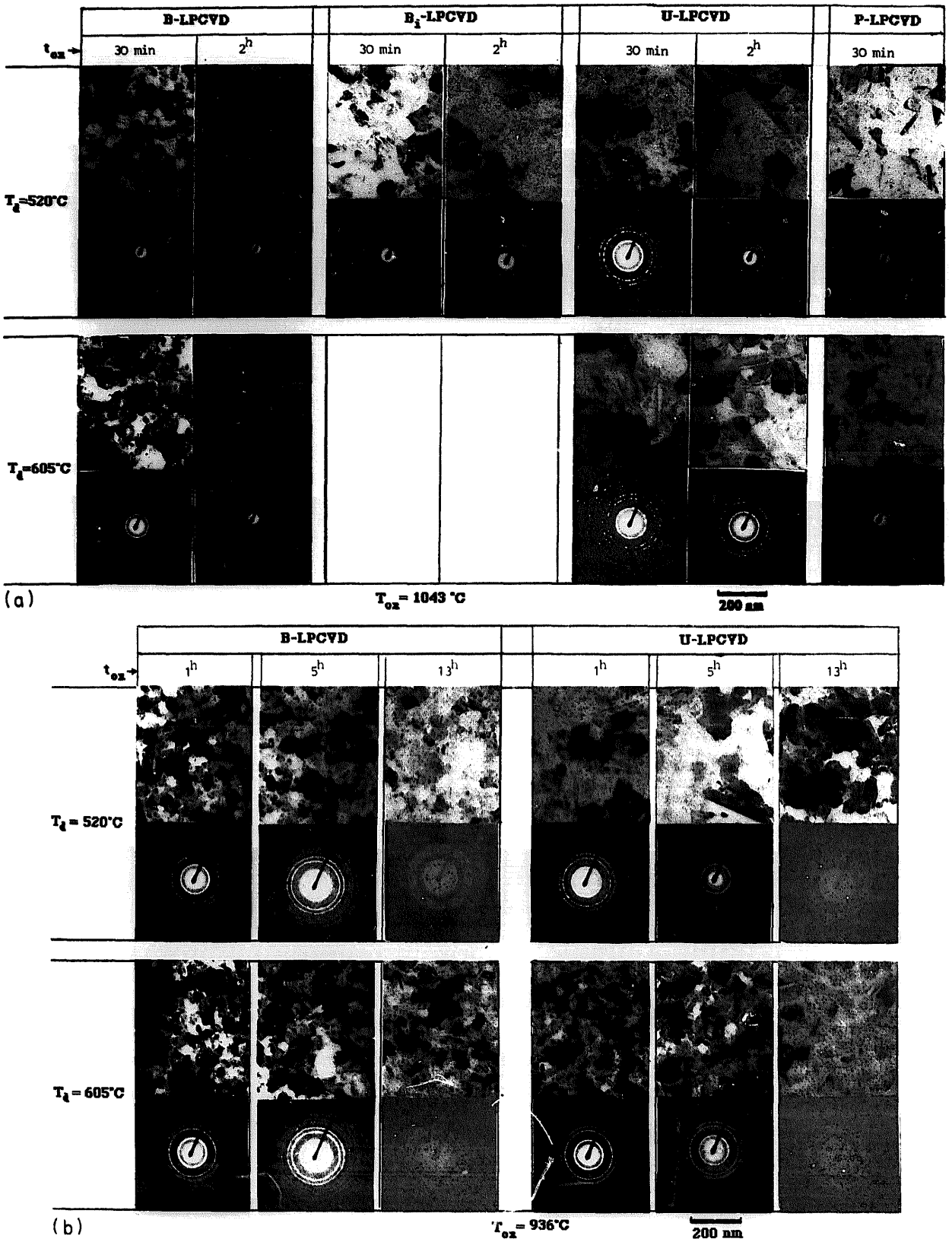

Fig. 7. Transmission electron micrographs and corresponding diffraction patterns of the four deposits: B-, B_i-, U- and P-LPCVD oxidized under dry O_2 at different oxidation temperatures T_{ox} = 1 043 °C (a) and T_{ox} = 936 °C (b) for the extremal deposited temperatures T_d = 520 °C and T_d = 605 °C. (Note: figure incomplete owing to damaged samples.)

oxidized at high temperature T_{ox} = 1 050 °C and for a long enough period (> 2 h) [11,18]. Simultaneously, as we can see from TEM observations on plane views as illustrated in (Fig. 7(a) and 7(b)), the film grain size tends to increase versus the thermal treatments. The weakest variation is noticed on the boron-doped films for a long time t_{ox} and high temperature T_{ox}; from 85 nm at (t_{ox} = 16 h, T_{ox} = 840 °C) to around 140 nm at (t_{ox} = 1 h 30 min, T_{ox} = 1 050 °C) when T_d = 520 °C. However, when T_d = {605–620 °C} this variation remains comparable. Thus, the largest grains ($\langle G \rangle_{max}$ = 200 nm wide) were observed in the oxidized films when these films are deposited at the highest temperature T_d = {605–620 °C}. The undoped films (Fig. 7(a) and 7(b)) show well-defined Si crystallites when T_d = 605 °C at T_{ox} = 936 °C, but misty grains or grains with blurred boundaries are observed at (t_{ox} = {30 min–5 h}, T_{ox} = {936–1 043 °C}) in the implanted and undoped films.

RHEED patterns associated with TEM observations show the preferred ⟨110⟩ texture for both undoped and boron-doped LPCVD silicon films, but a ⟨311⟩ preferred texture for the phosphorus-doped films. When the films evolve during the subsequent heat treatment, we will not be able to identify any noticeable changes of the initial texture observed.

In Fig. 8(a) and 8(b), we present the sheet resistivity measurements of B- and B_i-LPCVD layers, in which we show that the variations, with t_{ox} and T_{ox}, of the electrical resistivity of these two doped film series are also very different (Table 2). The resistivity value of the implanted films tends to increase above 5×10^{-3} Ω cm, while the value of the in-situ doped films tends to decrease below 5×10^{-3} Ω cm.

At this stage, the results presented in Figs. 1–6 and 8 regroup almost the whole features of thermal-oxidation mechanisms and then demonstrate that the higher crystalline quality (i.e. low defects and low doping densities) gives the lower oxidation rate of the polycrystalline films.

3.2. Mechanisms and kinetics of thermal oxidation

The values of W_{ox} as a function of (t_{ox}, T_{ox}) for the ⟨100⟩ monocrystalline test samples agree with those calculated from the models of Naïto et al. (two-oxide layers model) [7] or Han and Helms (two independent oxidizing species model) [8] without any modification of the oxidation parameters.

These models also give a good fit for the implanted ⟨100⟩-oriented control sample and for the various undoped films of the U-LPCVD series. On the other hand, the oxidation data of both the un-implanted and implanted ⟨111⟩-oriented samples are nicely fitted using a Deal–Grove-type model. If the first few minutes of the oxidation are excluded (these first minutes are usually characterized by very fast changes in the resistivity of all the doped film), a Deal–Grove-type model also suffices to simulate the oxidation of all the implanted or in-situ doped films.

Fig. 9 and Fig. 10 show changes in the fundamental oxidation parameters k_s and D, where k_s is the rate of the surface

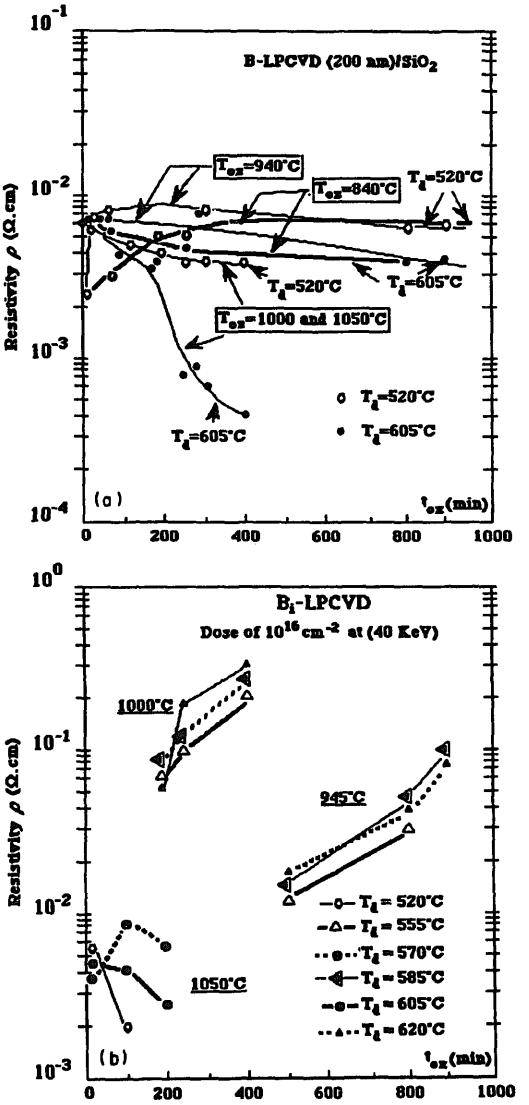

Fig. 8. Evolution of the average resistivity ρ as a function of oxidation time t_{ox} for the three oxidation temperatures T_{ox} = 840, 940 and 1 050 °C for the extremal deposited temperatures T_d = 520 °C and T_d = 620 °C: (a) for the B-LPCVD layers, (b) for the B_i-LPCVD layers.

oxidation reaction and D is the diffusion constant of the oxidizing species through the oxide deduced from the above simulations. k_s and D are respectively expressed by the two relations given below [9]:

$$B = 2\alpha D \text{ and } \frac{B}{A} = \alpha \frac{1}{k_s} + \beta \tag{3}$$

where $\alpha = C^*/N_1$, $\beta = \alpha/h$, in which C^* is the equilibrium concentration of the oxidizing species in the oxide film, h is the gas-phase mass-transfer coefficient, and N_1 is the number of oxidizing species incorporated into a unit volume of the oxide ($N_1 = 2.3 \times 10^{23}$ cm^{-3} for oxidation in dry oxygen [9]).

As we see, the linear rate constant B/A is associated with the reaction rate k_s at the oxide–silicon interface, and the parabolic rate constant B is also associated with the oxidizing species moving through the oxide layer D.

Table 2
Comparison between the mean four-point resistivity measurements (Ω cm) of the as-grown and B- and B_i-LPCVD silicon films annealed at T_{ox} = 840, 945, 1 000 and 1 050 °C for different durations t_{ox} and for the extremal deposited temperatures T_d = 520 and 605 °C

B-LPCVD	T_{ox} (°C)		840			945			1 050		
	t_{ox}		(1 h)	(4 h 35 min)	(16 h)	(12 min)	(1 h 46 min)	(13 h)	(12 min)	(1 h 30 min)	(4 h)
	ρ ($\times 10^{-3}$)	(ρ_{520})	3.4	5.0	6.3	5.3	7.5	6.0	5.5	6.0	5.0
		(ρ_{605})	5.3	4.0	3.8	7.2	6.5	3.0	6.0	6.0	1.0
As grown	(ρ_{520}) = 2.6×10^{-3}				(ρ_{605}) = 4.2×10^{-3}						
B_i-LPCVD	T_{ox} (°C)		945		1 000			1 050			
	t_{ox}		(9 h)	(16 h)	(3 h 10 min)	(4 h)	(6 h 45 min)	(30 min)	(2 h)	(3 h 15 min)	(4 h 33 min)
	ρ ($\times 10^{-3}$)	(ρ_{520})	14	3.0	50	100	200	5.7	2.0	4.0	25.0
		(ρ_{605})	18	95	40	100	300	4.3	3.6	2.4	55.0

In these results, both values of k_s and D are associated with the ⟨100⟩ monocrystalline test samples and correspond to the values of the oxidizing species 2 in the Han and Helms simulation. In this model, Han and Helms [8] introduced the concept of the parallel-oxidation regime, which is due to the presence of two independent oxidizing species diffusing in the oxide. This hypothesis yields an analytical expression of the global rate oxidation to be equal to the sum of two rates separately. The results in Figs. 9 and 10 clearly state the following.

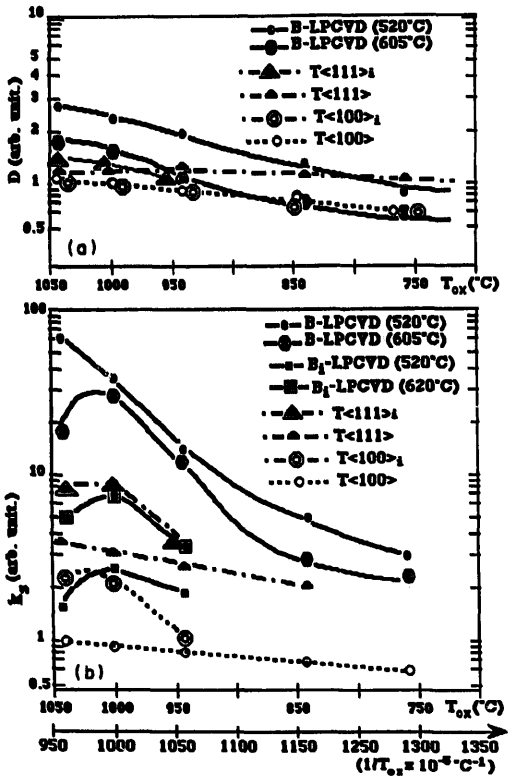

Fig. 9. (a) Diffusion constant D of the oxidizing species through the oxide and (b) the rate of the surface oxidation reaction k_s versus the inverse of the oxidation temperature ($1/T_{ox}$) of the two extreme deposited temperatures 520 to 605 or 620 °C of in-situ boron-doped B-LPCVD and boron-implanted B_i-LPCVD compared with the monocrystalline control samples T⟨100⟩, T⟨111⟩ and T⟨100⟩$_i$, T⟨111⟩$_i$ implanted.

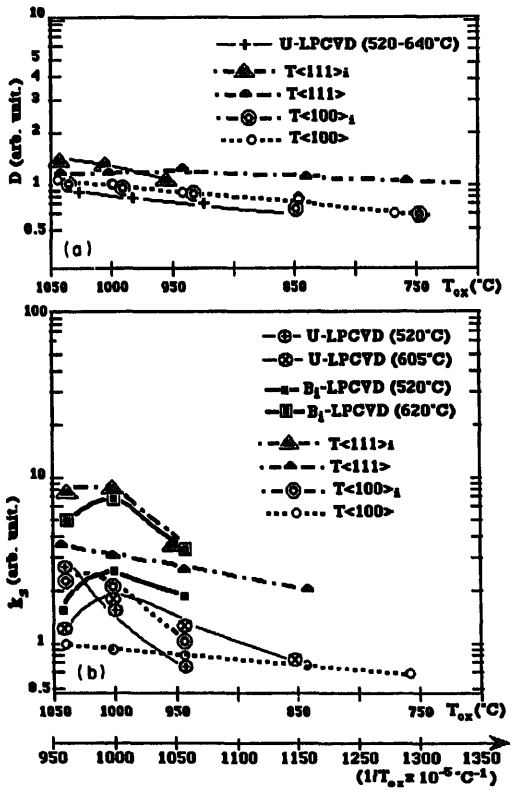

Fig. 10. (a) Diffusion constant D of the oxidizing species through the oxide and (b) the rate of the surface oxidation reaction k_s versus the inverse of the oxidation temperature ($1/T_{ox}$) of the two extreme deposited temperatures 520 to 605 or 620 °C of boron-implanted B_i-LPCVD and undoped U-LPCVD compared with the monocrystalline control samples T⟨100⟩, T⟨111⟩ and T⟨100⟩$_i$, T⟨111⟩$_i$ implanted.

1. The variation of the oxidation rates of the B-implanted films with T_d appears to be associated with the variations of the rate of the oxidation reaction at the film surface k_s (Figs. 9(b) and 10(b)).
2. Increases of both k_s and D cause the enhanced oxidation rate of the in-situ doped materials (Fig. 9(a) and 9(b)).

4. Discussion

The results of the thermal oxidation of heavily in-situ boron-doped films show that the oxidation rate is always too much higher than that of the similar doped single-crystal silicon. This strong oxidation is not found in the initially undoped or implanted layers. Whereas, this high oxidation is comparable with the heavily in-situ phosphorus-doped one, not only in magnitude, but also with the relative effect of dopant and to its dependency with the oxidation temperature T_{ox}.

We can understand that this enhancement in oxidation rate will correspond, at the same time, to the high values of the linear and parabolic rate constants. But these values themselves remain rather linked to the deposited conditions and to the initial crystalline structure of the deposits. In particular, the oxidation is too high when both the crystalline quality (i.e. Raman quality) and texture is poor.

Moreover, two oxidation temperature ranges seem to be established.

1. On one hand, $T_{ox} \leq 1\,000$ °C in which the energy activation values of the two linear and parabolic rate constants appear comparable with the ones found in heavily doped monocrystalline materials,
2. On the other hand, $T_{ox} > 1\,000$ °C, the energy activation values tend to present high values and seem to be in agreement with the reduced DOR effect observed in this range of T_{ox}.

If we refer to other published works [17,19], we can see that this enhancement of oxidation of B-LPCVD layers characterizes well the two basic phenomena specific to the thermal oxidation which are:

1. the oxide through the parabolic rate constant and also the diffusion constant D. This constant varies with the deposited conditions, but not with the conditions before annealing treatments (i.e. poly-Si cleaning samples steps and furnace input-output processes); and
2. the oxidation surface reaction through the linear rate constant and also the surface reaction constant k_s. This constant depends essentially on the treatment conditions.

The resistivity measurements, surface roughness, and TEM observation results seem to show that the effect of the surface reaction constant (more important in the first steps of oxidation) gives a weak evolution of boron concentration and surface roughness σ_a. On the contrary, it corresponds to a roughly variation of the resistivity ρ of the films and the grain average size $\langle G \rangle$. We note that the films deposited at low temperature $T_d = 520$ °C are characterized by a high enhancement of ρ_{520}, but with a small grain size $\langle G \rangle$, whereas, the deposited films at $T_d = 620$ °C present a totally opposite behaviour for which ρ_{605} decreases while $\langle G \rangle$ increases. Hence, after this stage of oxidation ρ_{520} becomes comparable with ρ_{605} and $\langle G_{520} \rangle$ tends to have a similar value to $\langle G_{605} \rangle$.

In general, it is found that the oxidation reaction decreases when the crystalline quality increases, which means the diminution of the density and disappearance of the intergranular region of the films, and the diminution of the boron supersaturation effect. This boron supersaturation effect yields the presence of metastable conjugate phase compounds such as SiB_x which causes a higher solid solubility limit with temperature treatments. More details of these effects phenomenon are given in Refs. [20,21,17].

As we can see, it is possible to explain this specific oxidation behaviour of the in-situ boron-doped films if we associate the supersaturation concentration effect which occurs at high boron-doping levels. The dopant concentration is itself proportional to the typical germination in the gaseous phase phenomenon occurring during the first growth steps of these films.

Also, we observe a significant difference between the evolution of the in-situ boron and phosphorus-doped films at the high oxidation temperature. This evolution with T_{ox}, which is in agreement with the one well-known evolution for the single-crystal silicon, shows an important excess and reaches a value of 25% instead of the 15% as expected in monocrystalline silicon doped at the same level. This may be explained by the fact that phosphorus doping beyond 4×10^{20} cm^{-3} [17] enhances grain growth, which is attributed to silicon self-diffusion through grain boundary enhancement with phosphorus concentration. In the case of boron doping, it is also seen that annealing at 1 000 °C increases mobility and grain size. These deposits possess a boron concentration lower than a saturation value at an annealing temperature and are assumed not to contain any precipitation. That is, grain growth is suppressed by the precipitation which is supposed to be at grain boundary and thus, may improve the crystalline quality of the films.

5. Conclusion

The study made shows that boron doping, and especially in-situ boron doping, strongly influences the thermal oxidation behaviour of the LPCVD-Si films some hundred nanometres thick. In particular, three major results have been put into evidence from which a large understanding of the film oxidation may be obtained.

1. In the case of the undoped films, the oxidation kinetics obeys a parallel oxidation model as does ⟨100⟩ monocrystalline silicon. However, the oxidation of both boron-implanted and in-situ doped films follows a single oxidizing species model for the Deal–Grove type, in the same way as the oxidation ⟨111⟩ monocrystalline materials.

2. From an oxidation kinetics simulation, it is shown that the oxidation of the implanted films is associated with the enhancement of the surface oxidation rate k_s, whose value increases with the film deposition temperature T_d.
3. By comparison, the oxidation of the in-situ doped films show typical features which are associated with their structural properties. The structural properties are mainly the defects, boron atom distribution in the crystalline grains, and intergrain regions of these deposit. We noticed also a very large increases of both k_s and D even when the film deposition temperature T_d decreases which is typical for the in-situ doped films.

Acknowledgements

We are indebted to A. Bounamis, A. Nouicer of the "Ecole Nationale Supérieure de Jijel (ENSJ)", also to the members of the LAAS-TEAM of Toulouse for their services and technical assistance, and for M. Barkat (MC) for his helpful suggestions.

References

[1] G. Queirolo, E. Servida, L. Baldi, G. Pignatel, A. Armigliato, S. Frabboni and F. Corticelli, *J. Electrochem. Soc.*, *137*(3) (1990) 967.
[2] K.C. Saraswat and H. Singh, *J. Electrochem. Soc.*, *129*(10) (1982) 2321.
[3] H. Sunami, *J. Electrochem. Soc.*, *125* (1978) 892.
[4] C.P. Ho and J.D. Plummer, *J. Electrochem. Soc.*, *126* (1979) 1516.
[5] C.P. Ho and J.D. Plummer, *J. Electrochem. Soc.*, *126* (1979) 1523.
[6] B.E. Deal and A.S. Grove, *J. Appl. Phys.*, *132* (1965) 2815.
[7] M. Naïto, H. Homma and N. Nossna, *Solid State Electron.*, *29* (1986) 885.
[8] C.J. Han and C.R. Helms, *J. Electrochem. Soc.*, *134* (1987) 1297.
[9] A.S. Grove, *Physics and Technology of Semiconductor Devices*, Wiley, New York, 1967, p. 27.
[10] J. Baudet and D. Bielle-daspet, *Internal Report of the LAAS of CNRS (France)*, No. 88227, 1988.
[11] D. Bielle-Daspet, E. Scheid, C. Azzaro, B. de Mauduit and B. Pieraggi, *Thin Solid Films*, *204* (1991) 33.
[12] D. Bielle-Daspet, L. Mercadere, M. Boukezzata, B. Pieraggi and B. de Mauduit, *Thin Solid Films*, *175* (1989) 43.
[13] L. Mercadère, F. Mansour-Bahloul, M. Boukezzata and D. Bielle-Daspet, *Proc. Int. Symp. on Trends and New Applications in Thin Films, Strasbourg, March 16–20 1987*, Société Française du Vide, Paris, Vol. 1, 1987, p. 183.
[14] D. Bielle-Daspet, A. Martinez F. Mansour, B. Pieraggi, M.J. David, B. de Mauduit, A. Oustry, R. Carles, J. Landa, F. Ajustron, A. Mazel and P. Riboulet, *Thin Solid Films*, *150* (1987) 69.
[15] D.M. Kim, F. Qian, *IEEE Trans. Electron Devices, ED-34*(8) (1987) 1774.
[16] J.Y.W. Seto, *J. Appl. Phys.*, *46*(12) (1975) 5247.
[17] T. Makino and H. Nakamura, *Solid State Electron*, *24* (1981) 49.
[18] M. Boukezzata, *Doctorate Thesis*, Université Paul Sabatier of Toulouse, France, No. 353, 1988.
[19] L. Mercaderre, *Doctorate Thesis*, I.N.S.A of Toulouse, France, No. 68, 1988.
[20] A. Armigliato, D. Nobili, P. Ostoja, M. Servidori and S. Solmi, *Semiconductor Silicon*, J. Electrochem. Soc., New York, 1977, pp. 638–647.
[21] E. Arai, H. Nakamura and Y. Terunuma, *J. Electrochem. Soc.*, *120* (1973) 980.